

# Power law relaxation and glassy dynamics in Lebwohl-Lasher model near isotropic-nematic phase transition

Suman Chakrabarty, Dwaipayan Chakrabarti, and Binan Bagchi

Solid State and Structural Chemistry Unit,  
Indian Institute of Science, Bangalore 560012, India.

(Dated: March 23, 2024)

Orientalional dynamics in a liquid crystalline system near the isotropic-nematic (I-N) phase transition is studied using Molecular Dynamics simulations of the well-known Lebwohl-Lasher (LL) model. As the I-N transition temperature is approached from the isotropic side, we find that the decay of the orientational time correlation functions (OTCF) slows down noticeably, giving rise to a power law decay at intermediate timescales. The angular velocity time correlation function also exhibits a rather pronounced power law decay near the I-N boundary. In the mean squared angular displacement at comparable timescales, we observe the emergence of a subdiffusive regime which is followed by a superdiffusive regime before the onset of the long-time diffusive behavior. We observe signature of dynamical heterogeneity through pronounced non-Gaussian behavior in orientational motion particularly at lower temperatures. This behavior closely resembles what is usually observed in supercooled liquids. We obtain the free energy as a function of orientational order parameter by the use of transition matrix Monte Carlo method. The free energy surface is flat for the system considered here and the barrier between isotropic and nematic phases is vanishingly small for this weakly first-order phase transition, hence allowing large scale, collective and correlated orientational density fluctuations. This might be responsible for the observed power law decay of the OTCFs.

## I. INTRODUCTION

Liquid crystalline systems often exhibit interesting dynamics apart from the rich phase behavior. Surprisingly, dynamics of such systems have traditionally been probed only at rather long timescales (nanoseconds to milliseconds) [1, 2, 3]. Recently, Fayer and coworkers have investigated the dynamics in the isotropic phase of thermotropic liquid crystals over a wide range of timescales using optical Kerr effect (OKE) measurements [4, 5, 6, 7]. At short to intermediate timescales, they have observed a pronounced power law decay of the time-dependent OKE signal near the I-N phase transition. At the intermediate times (several nanoseconds) the decay becomes even slower, almost appearing as a plateau on a log-log scale [4]. The exponential decay predicted by Landau-de Gennes theory is observed only at the longest timescale ( $> 10$  ns).

Subsequent molecular dynamics simulations of a calamitic system (comprising of rod-like molecules) with the Gay-Berne pair potential were found to reproduce the power law decay of orientational time correlation functions (OTCF) [8]. From a very recent computational study, which deals with a calamitic system, a discotic system (comprising of disc-like molecules) and to a limited extent the Lebwohl-Lasher lattice model, it appears that this power law decay at short-to-intermediate times might be a rather general phenomenon in thermotropic liquid crystals [9]. This observation has gained support from a recent finding of power law decay at relatively

short times in an idealized calamitic liquid crystal model with length-to-width ratio 5-6 [10]. It has been observed that many aspects of the orientational relaxation behavior outlined above bear close resemblance to what is observed in supercooled molecular liquids near the glass transition temperature [7, 9, 11]. In particular, the description of orientational relaxation with a power law decay at short times and exponential decay at long times is strikingly similar [7]. However, the origin of such a rich dynamical behavior may be quite different in the two cases [9]. It would be especially interesting to explore the free energy surface with respect to orientational density fluctuations in search of the origin of the slow dynamics near the I-N transition.

Comprehensive understanding of this rather exotic dynamics of thermotropic liquid crystals spread over almost five decades of time is a challenging task, particularly because of the anisotropic nature of the interaction, which makes the theoretical analysis difficult. Computational approaches have become very much useful in this regard as we gain control over the microscopic interactions and try to understand their manifestation into the macroscopic behavior. In this spirit, this communication attempts to continue the investigation of the Lebwohl-Lasher model.

Lebwohl-Lasher (LL) model [12] is essentially the lattice version of the Maier-Saupe model. In this model, the molecules being fixed on a simple cubic lattice lose their translational degrees of freedom and can only rotate. The total interaction energy is given as follows:

$$U = \frac{1}{2} \sum_{ij} \left( \frac{3}{2} \cos^2 \theta_{ij} - \frac{1}{2} \right) \quad (1)$$

where  $\theta_{ij}$  is the coupling parameter, signifying the strength of interaction between the rotors. It has a fixed

---

Electronic address: bbagchi@sscu.iisc.ernet.in; URL: <http://liquid.sscu.iisc.ernet.in/>

value for the nearest neighbors and 0 otherwise.

LL model has been rather popular since its inception in computer simulation studies of liquid crystals. Its merit lies in the inherent simplicity with which it clearly establishes some of the very essential features of orientational ordering in liquid crystalline systems [13, 14, 15, 16, 17]. Simple form of the anisotropic interaction and the absence of translational degrees of freedom makes the system particularly easy to study. Most of the earlier studies involving LL model used Monte Carlo (MC) methods, which can not predict the real dynamics of the system. In view of this, here we have undertaken molecular dynamics (MD) simulations to investigate the dynamics in the LL model.

Our MD simulations of the LL model show that as the transition temperature is approached from the isotropic side, the decay of the orientational time correlation functions slows down noticeably, giving rise to power law decay at intermediate time scales. Another interesting result is the emergence of subdiffusive orientational motion essentially in the same temporal window where the power law decay sets in. In addition, the subdiffusive motion is followed by a superdiffusive regime before the long-time diffusive behavior sets in. Moreover, we have used the recently developed transition matrix Monte Carlo (TMMC) method to obtain the free energy profile for the system as a function of orientational order parameter. We find the barrier to be vanishingly small for this weakly first-order transition allowing large fluctuations in the orientational order.

The organization of the rest of the paper is as follows. In the next section, we discuss the details of simulations. In section III, we present the results on orientational relaxation. Section IV deals with the TMMC method and the results it yields on the free energy calculation. Section V concludes with summary and a few pertinent comments.

## II. SIMULATION DETAILS

The system under study consists of a  $(10 \times 10 \times 10)$  simple cubic lattice with one rotor fixed on every lattice point. Only the nearest neighbors interact through the orientation dependent potential given by Eq. (1). Throughout we have used dimensionless temperature  $T$  and time  $\tau$  (for the MD studies) defined by [13]:

$$\begin{aligned} T &= k_B T = \\ \tau &= (\tau_0 / I_\perp)^{1/2} \end{aligned} \quad (2)$$

Here both the parameters  $\tau_0$  and  $I_\perp$  (moment of inertia with respect to the axis perpendicular to the molecular axis) have been taken to be unity.

We have performed Molecular Dynamics (MD) simulations in microcanonical (NVE) ensemble using velocity Verlet algorithm. We have used time step of  $\tau = 0.002$

in reduced unit and have obtained energy conservation upto fifth place of decimal throughout the simulation. We have scaled the velocities at every 100 steps for initial  $10^5$  steps to equilibrate the system at a particular desired temperature and stored the trajectory for analysis after allowing the system to evolve without scaling for another  $10^5$  steps. The standard deviation in temperature during data acquisition was of the order of 0.01 for all temperatures. Periodic Boundary Conditions (PBC) have been applied to remove the surface effects. Earlier MC studies showed pronounced system size dependence for this model. The same applies for the MD simulation also. The size effect is particularly important near the transition temperature as the correlation length tends to diverge. The transition becomes sharper with increasing system size. The transition temperature ( $T_{IN}$ ) and the free energy barrier follow certain finite size scaling laws [16]. We have found the dynamical features reported here to be qualitatively similar for different system sizes.

## III. RESULTS

The phase behavior for LL model has been well explored using Monte Carlo (MC) methods for pretty large systems. But since there are relatively less number of Molecular Dynamics (MD) studies, we have computed the average order parameter at various temperatures using MD trajectories. The value of orientational order parameter is determined by diagonalization of the ordering matrix  $Q$  [1, 17]:

$$Q = \frac{1}{2N} \sum_{i=1}^N [\mathbf{e}_i \mathbf{e}_i^T]; \quad (3)$$

where  $\mathbf{e}_i$  is the  $i$ -th Cartesian coordinate of the unit vector ( $\mathbf{e}_i$ ) specifying the orientation of the  $i$ -th molecule. The largest eigenvalue and corresponding eigenvector give the orientational order parameter and the director respectively for a particular configuration. The thermodynamic order parameter ( $S$ ) is obtained by averaging over the simulation trajectory. As shown in Fig. 1 the data obtained from the MD simulation overlaps well with the result obtained from our MC simulation.

Note that MD simulation gives us the value of the transition temperature to be  $T = 1.14$ . This differs from the more accurate value ( $T = 1.1232$ ) obtained from MC simulations [16, 18] at the second place of decimal. This is acceptable because of the fluctuation in temperature present in microcanonical (NVE) MD simulation and the standard deviation of the order of 0.01 at all temperatures. The fluctuation in temperature is particularly high near  $T_{IN}$ . We have used the value obtained from our MD simulation to explain our other observations.

Often the second rank order parameter is not enough to decide if true long range order exists in the system. For that purpose, orientational correlation functions ( $G_1(r)$ )

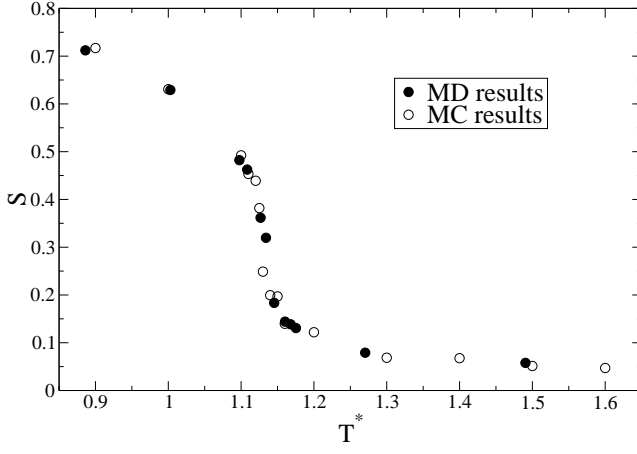


FIG. 1: The average orientational order parameter indicating the I-N transition at  $T^* = 1.14$ . Empty circles indicate the MC results and filled circles indicate the MD results.

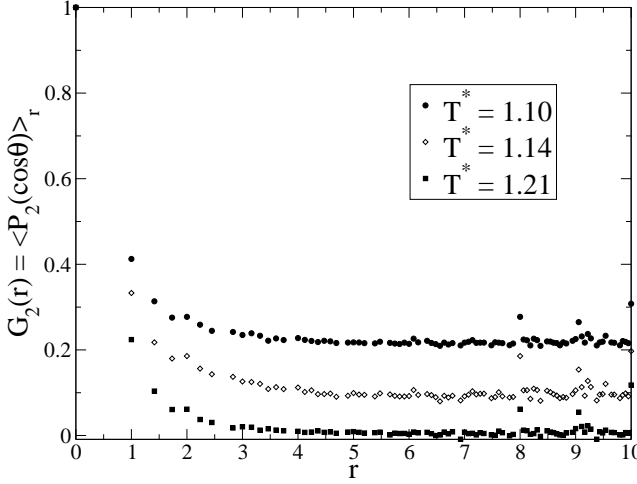


FIG. 2: The nature of spatial decay of the two particle orientational correlation function  $G_2(r)$  clearly demonstrates the existence of long range order in nematic phase. The correlation function decays to very small value as isotropic phase is reached.

are particularly useful. The set of correlations can be defined as expansion coefficients of the rotationally invariant pair distribution [17]:

$$G(r;_{12}) = G_0^{00}(r) \sum_1 \frac{2l+1}{64^{\frac{1}{2}}} G_l(r) P_l(\cos \theta_{ij}); \quad (4)$$

where  $G_0^{00}(r)$  is the particle center distribution,  $\theta_{ij}$  is the angle between rotors  $i$  and  $j$ , and  $P_l$  is the Legendre polynomial of rank  $l$ . For a simple cubic lattice,

$$G_0^{00}(r) = \frac{1}{4} \sum_k \frac{z_k}{r^2} z_k(r - r_k); \quad (5)$$

where  $\rho$  is the density and  $z_k$  is the number of neighbors at  $r_k$ . Hence,  $G_1(r) = \rho P_1(\cos \theta_{ij})_r$  gives orienta-

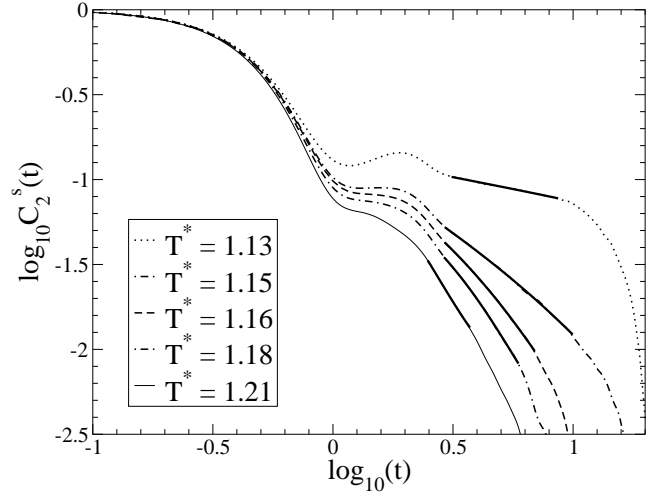


FIG. 3: Demonstration of power law regimes in the log-log plot of single particle orientational correlation function  $C_2^s(t)$ : Fitted power law regimes are shown in thick lines. The decay is almost exponential for the highest two temperatures, i.e. the power law component becomes very small.

tional correlation between two rotors separated by distance  $r$ . Figure 2 demonstrates that if true long range order is present,  $G_2(r)$  decays to a plateau with value  $\rho P_2$  [17].

#### A. Power law decay in OTCFs

Single particle OTCF gives a temporal measure of the loss of the memory of a single particle of its own orientation in the environment created by the surrounding molecules. The single particle OTCF of rank  $l$  is defined as:

$$C_l^s(t) = \frac{\langle \frac{1}{N} \sum_i P_l(e_i(0) \cdot e_i(t)) \rangle}{\langle \frac{1}{N} \sum_i P_l(e_i(0) \cdot e_i(0)) \rangle} \quad (6)$$

where  $e_i(t)$  is the unit vector denoting the orientation of  $i$ -th molecule at time  $t$ . Since LL model has up-down symmetry,  $C_2^s(t)$  would be physically meaningful.

In Fig. 3 the log-log plot of  $C_2^s(t)$  versus time is shown at different temperatures approaching  $T_{IN}$ . An interesting step-like decay is clearly evident. The power law behavior emerges just above the transition temperature, i.e. in the isotropic phase close to the I-N transition and continues in the nematic phase. It has been rather difficult to fit the entire decay by a single function due to the oscillatory regime in the nematic phase and rather dominant plateau appearing just before the power law regime. Hence, the OTCF has been fitted only beyond the initial plateau using the following functional form.

$$C_2^s(t) = A + \exp(-(t - t_p)^a) \quad (7)$$

Here, the parameter  $t_p$  gives the timescale corresponding to the long time exponential decay, the parameter  $p$

signifies the time scale of the power law decay and the parameter  $a$  gives the power law exponent. The values for  $\tau$ ,  $p$  and  $a$  are shown in the following table. Note that the nature of the decay of the single-particle OTCF is strikingly similar to the experimental results obtained by OKE measurements.

T		$p$	$a$
1.13	66.17	0.002	0.33
1.15	12.86	0.1	0.82
1.16	3.67	0.07	0.64
1.18	1.69	0.0	0.001
1.21	0.84	0.0	0.0

We have an interesting observation that the time scale of the exponential decay at the longer times becomes progressively larger with decreasing temperature, whereas the values of  $p$  clearly indicate that power law decay exists only near I-N phase boundary and this becomes transient as one moves away from the transition region. The values of the exponent  $a$  follows a similar trend. The OTCFs for the highest two temperatures are almost purely exponential beyond the plateau. We interpret the above result in the following fashion. As the temperature approaches  $T_{IN}$  from the isotropic side, the single particle orientational relaxation becomes slower due to the strong coupling of rotational motion with the surrounding molecules, which result in an orientational caging effect of the rotors. The formation of orientational cage or pseudo-nematic domains (within the isotropic phase) surrounding a molecule, gives rise to the retention of the memory of the previous orientation for a longer time, resulting in the slow relaxation process. Thus, the collective relaxation becomes important near the transition point.

Mode coupling theory (MCT) can be used to obtain a semi-quantitative theoretical description and also physical insight of the slow dynamics near phase transitions [19, 20, 21]. MCT starts with splitting the frequency ( $z$ ) dependent memory function, here the rotational friction, into two parts:

$$\Gamma(z) = \Gamma_B(z) + \Gamma_C(z) \quad (8)$$

where  $\Gamma_B(z)$  is the short range or binary part which decays on a short time scale and usually originates from collisions between the molecules. Whereas,  $\Gamma_C(z)$  is the collective part, deriving contribution from collective correlations.

In the present lattice model there is no collisional contribution to the rotational friction. Therefore,  $\Gamma_B(z)$  can be set to zero and this is in fact the reason for the large contribution of the initial inertial decay. Friction is small at short times. However,  $\Gamma_C(z)$  exhibits singular features at small frequencies due to the emergence of long range orientational correlations near the I-N phase boundary. It was shown elsewhere that at low frequency,

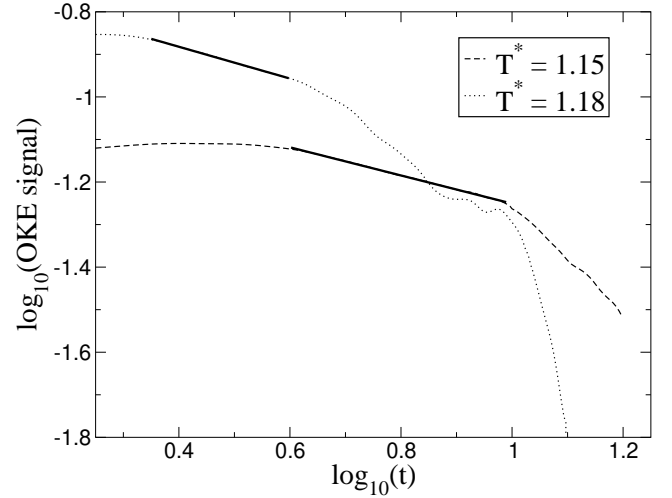


FIG. 4: Power law is exhibited in the derivative of collective OTCF, which is essentially the OKE signal. Fitted power law regimes are shown by thick lines.

the frequency dependent friction develops a rapid growth which can be represented as [4]:

$$\Gamma_C(z) \sim A z \quad (9)$$

Mean field treatment gives  $\nu = 0.5$ . In general, invoking the rank (1) dependence of the memory function, the single particle OTCF can be expressed as [22, 23, 24, 25]:

$$C_1^s(z) = \frac{1}{z} + \frac{(1+\nu)k_B T}{I(z + \nu(z))} \quad (10)$$

As discussed by Gottke et al, this expression can be Laplace inverted to obtain a power law decay in  $C_2^s(t)$  over a range of time scales [4]. Note that Eq. (9) is valid neither at large nor at very small  $z$ , rather at intermediate times.

To study the collective relaxation, we have calculated the collective OTCF defined as:

$$C_1^c(t) = \frac{\sum_i \sum_j P_i P_j \langle e_i(0) \cdot e_j(t) \rangle}{\sum_i \sum_j P_i P_j \langle e_i(0) \cdot e_j(0) \rangle} \quad (11)$$

Evidently, the calculation becomes computationally quite expensive even for a 1000 particle system.

Note that the time derivative of the collective OTCF is directly related to the time derivative of polarizability-polarizability correlation function and hence, to the OKE signal [4]. In Fig. 4 we show the prominent power law regimes in the log-log plot of derivative of  $C_2^c(t)$  at two temperatures just above  $T_{IN}$ . In the case of the collective OTCF, the power law exponents vary only little with temperature. The value of the exponents are 0.33 for  $T^* = 1.15$  and 0.37 for  $T^* = 1.18$ .

Experimental studies on liquid crystalline systems with rod-like molecules find the value of the power law exponent in the range of 0.6-0.7 [7]. As observed before, the values of the exponent  $a$  are not universal.

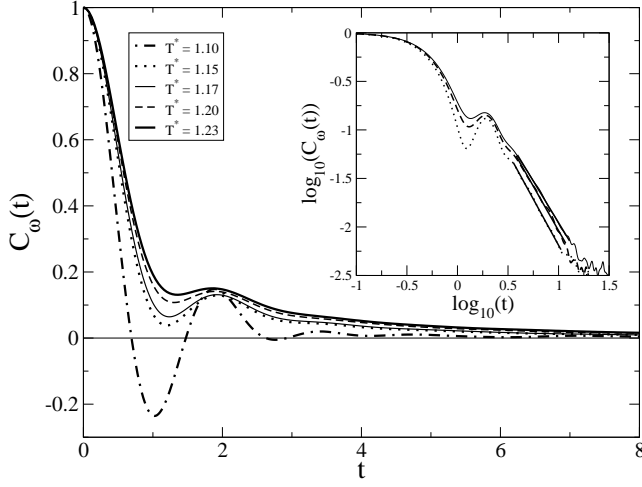


FIG. 5: Power law is exhibited in the angular velocity autocorrelation function at various temperatures across I-N phase transition. Inset figure shows the log-log plot for three temperatures and the thick lines indicate the linear fits obtained in power law regimes.

#### B. Power law decay in angular velocity autocorrelation function

We have calculated the angular velocity autocorrelation function  $\langle C_\omega(t) \rangle$  defined as:

$$\langle C_\omega(t) \rangle = \frac{\langle \mathbf{h}^\perp(0) \cdot \mathbf{h}^\perp(t) \rangle}{\langle \mathbf{h}^\perp(0) \cdot \mathbf{h}^\perp(0) \rangle} \quad (12)$$

where the angular velocity  $\mathbf{h}^\perp(t)$  is perpendicular to the axis of the rotor. In Fig. 5 we have shown the behavior of  $\langle C_\omega(t) \rangle$  at different temperatures near  $T_{IN}$ . We find that  $\langle C_\omega(t) \rangle$  has an oscillatory feature at short time scale due to the underdamped nature of the system. But we observe a pronounced power law decay with the value of the exponent being in the range of 1.7-1.8 at longer time scales. The origin of this power law can be attributed to the collective and correlated orientational density fluctuations.

As in the case of orientational correlation function  $C_2^s(t)$ , a semi-quantitative understanding of  $\langle C_\omega(t) \rangle$  can be obtained from MCT. Since the rotational friction is given by Eq. (9), we have the following approximate expression for  $\langle C_\omega(z) \rangle$ :

$$\langle C_\omega(z) \rangle = \frac{k_B T}{I(z + A z^{-1})} \quad (13)$$

This expression also gives rise to the power law decay of  $\langle C_\omega(t) \rangle$  at long times. Note that decay of  $\langle C_\omega(t) \rangle$  occurs at shorter times than that of  $C_2^s(t)$ . This is the reason for lower amplitude of power law decay in  $\langle C_\omega(t) \rangle$ .

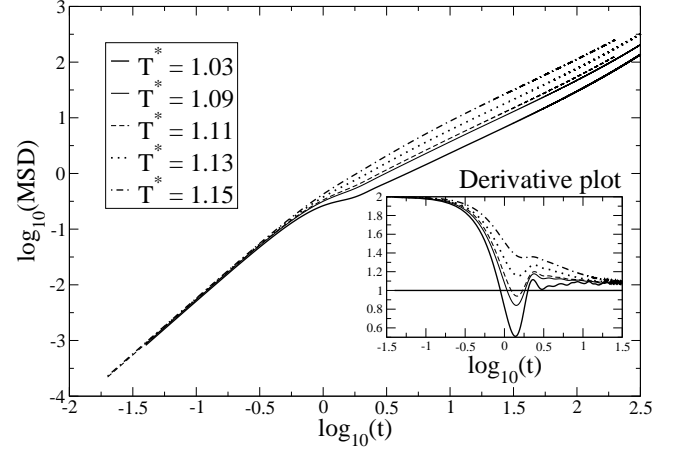


FIG. 6: The log-log plot of the rotational mean square displacement shows the gradual onset of subdiffusive regime followed by a superdiffusive jump as temperature is lowered across I-N phase boundary. The derivative of the same plot has been shown in the inset figure to clearly demonstrate the striking behavior. At very long time the derivative should converge to 1 corresponding to the diffusive limit.

#### C. Rotational diffusion

To probe the origin of the slow dynamics near the I-N transition, we have studied the rotational diffusion of the rotors on the lattice. The rotational displacement has been computed by integrating the angular velocity to have an unbounded representation [11, 26].

$$\tilde{\mathbf{r}}_n(t) - \tilde{\mathbf{r}}_n(0) = \int_0^t dt \mathbf{h}_n(t) \quad (14)$$

In Fig. 6 the log-log plot of the mean squared angular displacement versus time has been shown. Interestingly, we observe the emergence of a subdiffusive regime at a time scale comparable to the plateau observed in single particle OTCF. This behavior becomes apparent even in the isotropic phase and has been illustrated by the dip in the derivative of the log-log plot (inset of Fig. 6). The derivative plot shoots up suddenly after the dip and the motion remains superdiffusive. The system takes considerably long time to attain the diffusive limit. Our simulation has not been long enough to produce good averaging in that domain. Note that this subdiffusive behavior is well known in supercooled liquids and also has been found in calamitic systems studied with the Gay-Berne pair potential [11].

#### D. Non-Gaussian parameter

Non-Gaussian parameters (NGP) are often useful for description of the dynamical heterogeneity in complex systems [26, 27]. For a system with linear rotors, the

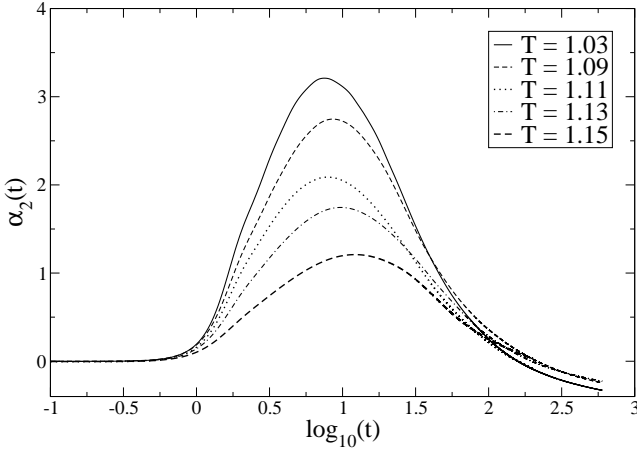


FIG. 7: The rotational non-Gaussian parameter across IN transition shows the increasing non-Gaussian behavior in the nematic phase. We don't observe any appreciable regular shift of the maximum with temperature as in supercooled liquids.

rotational NGP can be defined as [11, 26, 27]:

$$\alpha_2 = \frac{h}{2h} \frac{\langle t^4 \rangle}{\langle t^2 \rangle^2} - 1; \quad (15)$$

where

$$h \langle t^{2n} \rangle = \frac{1}{N} \sum_{i=1}^N h \tilde{j}_n(t) \tilde{j}_n(0) j_n^2 i \quad (16)$$

In Fig. 7 we show the time evolution of the rotational NGP. We observe large non-Gaussian behavior at intermediate timescales particularly at lower temperatures. Initially, when the motion of the rotors is ballistic, the rotational NGP is uniformly zero. It starts to grow at the comparable timescale as the appearance of the subdiffusive motion and the maximum is reached when the rotors escape from the orientational cage and gradually reaches the diffusive limit at longer timescales. The formation of pseudo-nematic domains as  $T_{IN}$  is approached from above would make the system dynamically heterogeneous. The growing peak in  $\alpha_2(t)$  can, therefore, be ascribed to the formation of pseudo-nematic domains. Note that similar behavior is well known in supercooled liquids [11, 26, 27, 28] and has been shown to be present in lattice models, e.g. in relaxation of phenomenological Brownian rotors based on the densely frustrated XY model [29]. However, we do not observe any regular shift in the position of the maximum within the temperature range of our consideration.

#### IV. FREE ENERGY AS A FUNCTION OF ORDER PARAMETER ( $S$ )

We have computed the free energy per rotor as a function of orientational order parameter using a variant of

transition matrix Monte Carlo (TM-MC) method recently proposed by Fitzgerald et al [30]. This method is considerably different than the reweighting methods for calculation of free energy and can be incorporated in any existing Monte Carlo simulation. An outline of the TM-MC method applied to the present problem follows.

The basic idea is to calculate the probability ( $S; \lambda$ ) that the system is in a macrostate  $S$  (in our case, average orientational order parameter) at the inverse temperature  $\lambda$ . Note that any average observable of the system can be computed once the macrostate probability is known, e.g. in canonical ensemble, the free energy can be obtained as a function of order parameter from

$F(S; \lambda) = -\ln(S; \lambda)$ . The Boltzmann macrostate probability can be expressed as  $(S; \lambda) = \sum_{s \in S} (s; \lambda)$ , where  $(s; \lambda)$  is the Boltzmann probability for a particular microstate (microscopic configuration)  $s$ . It is given by  $(s; \lambda) = \exp(-\lambda H_s)$ , where  $H_s$  is the value of the Hamiltonian for the microstate  $s$ .

The algorithm of finding  $(S; \lambda)$  is as follows:

1. Similar to Metropolis algorithm, for a given initial microstate  $s$ , a new state  $t$  is proposed with probability  $q_{s \rightarrow t}$ . As a simplification, we chose  $q_{t \rightarrow s} = q_{s \rightarrow t}$  though it is not strictly necessary.
2. The probability of the move to state  $t$  being accepted is

$$r_{s \rightarrow t}(\lambda; S) = \min\left(1, \frac{\exp(-\lambda H_t) (t; \lambda)}{\exp(-\lambda H_s) (s; \lambda)} g; \right) \quad (17)$$

where  $g_s$  is the weight function corresponding to macrostate  $S$ . For our purpose, we have set  $g_s = \ln(S; \lambda)$ , which corresponds to the multicanonical approach [30]. Thus the macrostates with lower probability are given more weight so that toward the end of the simulation the histogram becomes flat and low probability states are sampled quite well.

3. A new bookkeeping step is incorporated following the equilibration of the above Markov chain. At every step an array  $C_{S;T}$  (initialized to zero) is incremented as follows:

For  $S \neq T$ ,

$$\begin{aligned} C_{S;T}(\lambda) &= C_{S;T}(\lambda) + r_{s \rightarrow t}(\lambda; S) \\ C_{S;S}(\lambda) &= C_{S;S}(\lambda) + (1 - r_{s \rightarrow t}(\lambda; S)) \end{aligned} \quad (18)$$

For  $S = T$ ,  $C_{S;S} = C_{S;S} + 1$ . Note that while the Markov chain is guided by the multicanonical weight, the unweighted Boltzmann transition probabilities are stored for each visited macrostate.

The canonical transition probability (CTP) between the macrostates has been calculated at some interval as

$$P_{S;T}(\lambda) = \frac{C_{S;T}(\lambda)}{\sum_U C_{S;U}(\lambda)} \quad (19)$$

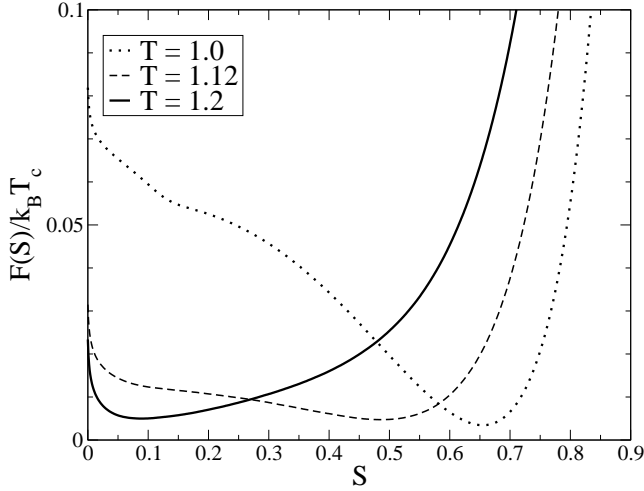


FIG. 8: Free energy versus order parameter plot for a 10 × 10 system at three different temperatures.

The equilibrated Markov chain must obey the detailed balance equation  $\pi(S)P_{S,T}(S') = \pi(T)P_{T,S}(S)$ . Hence, the macrostate probabilities have been obtained by solving the set of coupled linear equations iteratively. The weights have been updated at every 150  $L^3$  steps and the simulations have been continued for  $5 \times 10^6 L^3$  steps. The system learned to pass through the low probability states automatically and reasonably good sampling was attained.

The computed free energy surface is shown in Fig. 8. The flatness of the free energy surface near  $T_N$  is certainly a consequence of the very weakly first order nature of the transition and also partly due to the finite size of the system [16]. Thus, a system of this size exhibits large scale fluctuation in the value of the orientational order parameter. Such fluctuations can give rise to the power law decay in OTCFs [9]. As the system size increases, a small barrier separating the isotropic and nematic phases appears near the critical point [16]. This barrier height is directly related to the surface tension between the isotropic and the nematic phases and it follows a finite size scaling law [16, 30, 31]:

$$\frac{F_s}{k_B T} = \lim_{L \rightarrow \infty} \frac{1}{2L^{d-1}} \ln \frac{\pi_{\max}(S)}{\pi_{\min}(S)}; \quad (20)$$

where  $F_s$  is the surface free energy,  $d$  is the dimension,  $L$  is the box length, and  $\pi_{\max}(S)$  and  $\pi_{\min}(S)$  correspond to the maximum and minimum values of macrostate probability respectively.

Our result for 1000-particle system differs from one of the earlier reports [16], which uses Ferrenberg-Swendsen reweighting technique, as the positions of the minima are comparatively well-separated in our case while we consider temperatures far away from  $T_{IN}$ . We feel this has better agreement with the average order parameter values that one should obtain at those temperatures. But for complete comparison between the methods and to

verify the scaling relations for free energy barrier, more detailed study in larger systems is necessary.

It was discussed previously that the nearly flat free energy surface can be included in a Ginzburg-Landau type free energy functional [9]. One can then write down the following generalized Langevin equation for the fluctuating nonconserved order parameter  $(S)$  [9, 20]:

$$\frac{d(S)}{dt} = -\gamma \frac{\delta F(S)}{\delta S} + R(t); \quad (21)$$

where  $\gamma$  is a damping coefficient,  $F(S)$  is the Landau-de Gennes free energy as a function of the orientational order parameter and  $R(t)$  is a random velocity term related to  $\gamma$  by the fluctuation-dissipation theorem. As the temperature approaches the critical temperature  $T_c$ , the free energy surface becomes soft. If one uses the Landau free energy expansion

$$F = A(T)(S)^2 + B(T)(S)^3 + C(T)(S)^4; \quad (22)$$

then it can be shown that Eq. 21 can give rise to a power law decay of  $\frac{\langle S(t) \rangle - \langle S(0) \rangle}{\langle S(0) \rangle}$  at short to intermediate times.

If the noise term in Eq. (21) is neglected and a Markovian approximation is made of  $\langle S(t) \rangle$ , then one finds a power law in the decay of  $\langle S(t) \rangle - \langle S(0) \rangle$ . This power law originates from the cubic and the quartic terms in the free energy expansion given in Eq. (22). However, an analytic solution in presence of the noise term  $R(t)$  becomes highly non-trivial and needs to be carried out numerically. Work in this direction is in progress.

There are, however, two limits where one can obtain semi-quantitative answer directly. If the free energy surface is nearly flat, as shown in Fig. 8, then decay of  $\langle S(t) \rangle - \langle S(0) \rangle$  occurs via a generalized diffusion. In this case, the power law decay originates from power law behavior (in time or frequency) of  $\langle S(t) \rangle$ . Note that flatness of free energy surface implies that  $A(T) \rightarrow 0$  near  $T_c$ . A study of relaxation by diffusion with a non-Markovian memory function was reported by Denny et al [32]. The alternate limit is where a significant barrier develops between the isotropic and the nematic phases. This, however, is expected to give largely an exponential decay.

Note that the Landau-de Gennes behavior is obtained by keeping only the quadratic term in Eq. (22) and the relaxation time is given by (in present notation):

$$\tau_{dG} = \frac{1}{2\gamma A(T)} \quad (23)$$

The exponential relaxation observed both in experiments and simulations follow the Landau-de Gennes behavior with time constant given by Eq. (23).

## V. CONCLUSION

This report contains to the best of our knowledge the first detailed study of dynamics in LL model near the

isotropic-nematic transition in the context of power law relaxation. Despite having a very simple intermolecular potential and no translational degrees of freedom, the LL model exhibits an array of interesting dynamical features near the I-N phase boundary. The orientational relaxation slows down at intermediate timescales possibly due to the caging effect produced by neighboring sites and formation of pseudo-nematic domains in the isotropic phase very close to  $T_{IN}$ . The caging causes the rotors to show subdiffusive behavior. But the caging is not strong enough and the system remains underdamped over a long period of time. Essentially this leads to the vanishingly small free energy barrier separating the isotropic and the nematic phases confirming the nature of the phase transition to be very weakly first order.

It is interesting to note the synergy in the emergence of the power law decay in orientational relaxation and the subdiffusive behavior of the rotational diffusion. It is also equally interesting to find the superdiffusive behavior that follows the subdiffusive behavior. This signifies the long flights of the rotors just after they escape from the cage.

The analogy between the relaxation in supercooled liquids and that in the isotropic phase near the I-N phase transition has been discussed only in recent literature [7, 11, 33]. Even the present simple model shows dynamic signatures which are well-known in supercooled liquids. Prominent among them, are the power law relaxation and the subdiffusive behavior. It is interesting to compare with the scenario in supercooled liquid where one often finds two power laws, one leading towards the plateau and the second one (Von Schweidler law) at longer times moving away from the plateau [7]. However, the origin of such analogous behavior in the two systems can be quite different. In the case of liquid crystals, the onset of long range orientational correlations and the formation of pseudo-nematic domains are responsible for the power law. Anomalies in the relaxation behavior

in supercooled liquids, on the other hand, are believed to have kinetic origin.

There now appear to exist two somewhat different interpretations of the power law decay. The first one, proposed by Gottke et al [4, 5], is in terms of diverging orientational pair correlation function giving rise to a power law divergence of the memory function at low frequency (Eq. (9)). The alternative explanation offered recently by Bagchi and coworkers [9], invokes large scale fluctuations in collective orientational density. The first explanation (in the spirit of MCT) does not require such large scale density fluctuation. It does, however, invoke diverging correlation length. The second explanation is particularly relevant for weakly first order transitions with second order characteristics where the two phases are separated by low barrier.

Because of the length of the MD simulations required to obtain a reliable, statistically significant power law decay, we have been limited to study a 1000-particle system. The underdamped nature of the relaxation has made the statistical averaging demanding. However, it would be worthwhile to consider larger systems. We have made preliminary study of a  $(20 \times 20 \times 20)$  lattice system (8000 particles). We find that the relaxation behavior does not change significantly, but the free energy surface starts showing the formation of a noticeable (but still small) barrier at the intermediate values of the order parameter as expected [16].

#### Acknowledgments

It is a pleasure to thank Dr. P. P. Jose and Dr. P. Bhimalapuram for helpful discussions. This work was supported in part by grants from DST, India and CSIR, India. S. C. and D. C. acknowledge CSIR, India and UGC, India, respectively, for providing financial support.

- 
- [1] P. G. de Gennes and J. Prost, *The Physics of Liquid Crystals* (Clarendon Press, Oxford, 1993), 2nd ed.
  - [2] S. Chandrasekhar, *Liquid Crystals* (Cambridge University Press, Cambridge, 1992).
  - [3] P. Oswald and P. Pieranski, *Nematic and Cholesteric Liquid Crystals* (CRC Press, Taylor and Francis Group, 2005).
  - [4] S. D. Gottke, D. D. B. Race, H. C. Ang, B. Bagchi, and M. D. Fayer, *J. Chem. Phys.* 116, 360 (2002).
  - [5] S. D. Gottke, H. C. Ang, B. Bagchi, and M. D. Fayer, *J. Chem. Phys.* 116, 6339 (2002).
  - [6] H. C. Ang, J. Li, and M. D. Fayer, *Chem. Phys. Lett.* 366, 82 (2002).
  - [7] H. C. Ang, J. Li, V. N. Novikov, and M. D. Fayer, *J. Chem. Phys.* 118, 9303 (2003).
  - [8] P. P. Jose and B. Bagchi, *J. Chem. Phys.* 120, 11256 (2004).
  - [9] D. Chakrabarti, P. P. Jose, S. Chakrabarty, and B. Bagchi, *Phys. Rev. Lett.* 95, 197801 (2005).
  - [10] D. Bertolini, G. Cinacchi, L. D. Gaetani, and A. Tani, *J. Phys. Chem. B* 109, 24480 (2005).
  - [11] P. P. Jose, D. Chakrabarti, and B. Bagchi, *Phys. Rev. E* 71, 030701(R) (2005).
  - [12] P. A. Lebwohl and G. Lasher, *Phys. Rev. A* 6, 426 (1972).
  - [13] C. Zannoni and M. Guerra, *Mol. Phys.* 44, 849 (1981).
  - [14] C. G. Bac, P. V. Ricardo, V. R. Carlos, M. D. Emesto, and A. Hasmy, *Phys. Rev. E* 63, 042701 (2001).
  - [15] C. W. Geer and M. A. Lee, *Phys. Rev. E* 49, 3225 (1994).
  - [16] Z. Zhang, O. G. Mouritsen, and M. J. Zuckermann, *Phys. Rev. Lett.* 69, 2803 (1992).
  - [17] P. Pasini and C. Zannoni, eds., *Advances in the Computer Simulations of Liquid Crystals* (Kluwer Academic Publishers, Dordrecht, The Netherlands, 2000).
  - [18] U. Fabbri and C. Zannoni, *Mol. Phys.* 58, 763 (1986).
  - [19] S. K. Ma and G. F. Mazenko, *Phys. Rev. B* 11, 4077 (1975).



- [20] P. C. Hohenberg and B. I. Halperin, *Rev. Mod. Phys.* 49, 435 (1977).
- [21] B. Bagchi and S. Bhattacharyya, *Adv. Chem. Phys.* 116, 67 (2001).
- [22] S. Ravichandran and B. Bagchi, *Int. Rev. Phys. Chem.* 14, 271 (1995).
- [23] B. Bagchi and A. Chandra, *Adv. Chem. Phys.* 80, 1 (1991).
- [24] J. B. Hubbard and P. G. Wolynes, *J. Chem. Phys.* 69, 998 (1978).
- [25] B. Bagchi, *J. Mol. Liq.* 77, 177 (1998).
- [26] S. Kammmerer, W. Kob, and R. Schilling, *Phys. Rev. E* 56, 5450 (1997).
- [27] C. D. Michele and D. Leporini, *Phys. Rev. E* 63, 036702 (2001).
- [28] W. Kob and H. C. Andersen, *Phys. Rev. E* 51, 4626 (1995).
- [29] S. J. Lee and B. Kim, *Phys. Rev. E* 60, 1503 (1999).
- [30] M. Fitzgerald, R. R. Picard, and R. N. Silver, *Europhys. Lett.* 46, 282 (1999).
- [31] K. Binder, *Phys. Rev. A* 25, 1699 (1982).
- [32] R. A. Denny and B. Bagchi, *J. Phys. Chem. A* 103, 9061 (1999).
- [33] J. Li, H. Cang, H. C. Andersen, and M. D. Fayer, *J. Chem. Phys.* 124, 014902 (2006).